Development of microstructure in nanostructures and thin films

Max O. Bloomfield[a], Yeon Ho Im[a], Jian Wang[b], Hanchen Huang[b], and Timothy S. Cale[a]

[a]Focus Center–New York: Rensselaer: Interconnections for Gigascale Integration
[b]Department of Mechanical, Aeronautical and Nuclear Engineering

Rensselaer Polytechnic Institute, Troy, NY 12180

ABSTRACT

We have created a finite-element based, multiple-material, levelset-based code to implicitly represent and track evolving islands and grains. With this method, the code can track island growth in three dimensions through nucleation to coalescence into a grain structure. We discuss the numerical methods, capabilities, and limitations of the code, and then examine the microstructures that result from different models of growth based on starting structures derived from atomistic Monte Carlo simulations. We show simulation results from a kinetically limited process (electroless deposition), a transport-limited process (physical vapor deposition), and a process neither transport nor kinetically limited (physical vapor deposition with orientation dependent sticking factors).

1. INTRODUCTION

Thin films are critical to the performance of many products. For example, progress in IC performance has been largely driven by the ability to fabricate smaller devices and circuits. Process engineers have worked towards understanding thin film deposition processes, as well as properties of the deposited films; *e.g.*, thickness uniformity, electrical and mechanical properties, and crystallographic texture. As film thicknesses and the size of the features onto which the films are deposited continue to decrease in microelectronics applications, the underlying microstructure of these, often polycrystalline, films has become increasingly important. A recent study of copper electroplating baths reported copper grain sizes ranging from 0.1 to 0.25 μm for a widely used electrolyte [1]. With the state of the art in copper interconnect technologies for integrated circuits reaching this size scale [2], the grain structures of these films can have a large impact on reliability [3], manufactureability [4], and performance of those circuits [5].

Significant effort has been made to simulate the development of grain structures. Much work has been done in both two- and three-dimensional systems, using a variety of methods, including Potts models [6, 7], phase field models [8], molecular dynamics methods [9] and kinetic lattice Monte Carlo (KLMC) techniques [10–12]. Some of the most successful simulation techniques for grain structure modeling involve representing discrete entities, usually associated with atoms or aggregates of atoms. Such discrete representations, while natural at smaller scales, can become unwieldy at larger scales, as the number of discrete particles increases beyond what can be easily handled by modern computers.

Fully continuum representations do not have this particular limitation of having a length scale built in through a particle size. This makes such representations attractive; however, representing the physics in a reasonable manner may require information that comes from the discrete nature of the material, on both atomistic and grain scales. Thus, we combine discrete and continuum representations in the so-called “grain continuum” representation, which treats individual grains as continua, but treats them as distinct from each other. Additionally, there is a need for tools that allow us to recover atomistic level data locally, to get property information from the atomic scale structure, as appropriate.

Perhaps the most obvious way to approach this grain-continuum type of representation is through an explicit representation of the boundaries, by either segments in 2D or polygons in 3D. Frost and Thompson [13] and Frost *et al.* [14] used such an explicit front-tracking method in 2D to study the evolution of grain size distributions. Zhang and Adams developed `FACET` [15], which explicitly tracks grains boundaries and surfaces in 2D through the use of line segments. Roosen and Carter [16] also performed grain development simulations on polygonal grains, using explicit representations to simulate coarsening. Kuprat [17] reported on an explicit, 3D, moving boundary grain structure evolution code `GRAIN3D` that uses the Las Alamos Grid Toolbox (`LaGriT`) [18], and demonstrated it for grain boundary motion under mean curvature [17]. Many complex operations are involved with maintaining the mesh topology during explicit evolution [19–23].

Nanotechnology, Robert Vajtai, Xavier Aymerich, Laszlo B. Kish, Angel Rubio, Editors,
Proceedings of SPIE Vol. 5118 (2003) © 2003 SPIE · 0277-786X/03/$15.00

Because of the difficulty of explicit front tracking in 3D, interface tracking is often done using a levelset method in a variety of applications, including computer vision, multiphase flow, and pattern recognition [24, 25]. Using levelset-based grain-continuum representations, we have created a software tool, the parallel levelset environment for nanoscale topography evolution (PLENTE), which can be used to track grain structure development and evolution in fully three-dimensional systems, but can take structural inputs from discrete methods, such as as KLMC simulations.

Built into PLENTE are routines to "encapsulate" discrete representations of structure, taken either experimentally or from simulation. Once encapsulation is complete, and the structure is embedded in a grain-continuum representation, various types of process models or grain evolution models may be used with PLENTE to study how the system's geometry evolves in time. The numerical methods to accomplish this are discussed briefly in section 2, and the interested reader can consult Reference 26 and references therein. We have used PLENTE with several process models, including models for electroless plating (ELD) and physical vapor deposition (PVD) and in section 3, we show sample results from these processes.

2. NUMERICAL METHODS

In this section, we briefly discuss the numerical methods used to encapsulate atomistic data and to represent and evolve systems of grains under process models. An in-depth discussion of the technique may be found in Reference 26.

2.1. Levelset Representation

PLENTE is a grain-continuum method, which uses a grain-based, multiple levelset method, similar to those in Ref. 27. Levelset methods are based upon representing an interface implicitly, as a contour or "levelset" in a scalar field, and reducing explicit motion of the interface [28, 29] to the time evolution of the scalar field under a partial differential equation [24, 25]. The computational overhead of representing a field in n dimensions to track a $(n-1)$ dimensional interface is deemed to be made up for by not having to deal explicitly with several geometrically troublesome issues, such as topological changes in the structure. When tracking only two phases, it is convenient to use the zero contour of a single scalar field, φ, to indicate the position of the interface between them, using the sign of φ to indicate the "inside" versus "outside" of a particular phase. As a grain-based levelset simulator, PLENTE must be able to track multiple grains and allow them interact when the represented materials make contact and form material boundaries. We associate one levelset field variable or "φ" with each distinct material. Figure 1 illustrates the two-phase convention using one φ and the many-phase convention that we employ, setting $\varphi_i < 0$ for the inside of the ith phase.

During levelset calculations, the φ's are almost always chosen to be initialized to the signed distance from the interface [24,25]. This choice of fields has many desireable properties, including that it has its zero contour along the interface, that its contours are equispaced, and that the various derivatives of the fields can be equated to physical quantities, such as curvature and surface normal. The φ-fields are most often represented on a tensor-product grid, but we use linear finite elements on an unstructured mesh to represent and evolve the fields, reverting to tensor-product grids for some sub-tasks, such as re-initialization, as discussed below.

The resolution of a levelset representation is of the order of the size of the underlying mesh or grid elements for first order representations [25, 30]. Corners tend to round, and sharp points and cracks thinner than typical mesh and grid sizes can be eliminated completely. We have chosen to use the finite element based levelset representation on an unstructured mesh, in part, to address this issue. This representation lends itself to local spatial and polynomial refinement of the underlying discretization, in order to add precision in regions where it is important, such as near grain boundaries and triple points.

PLENTE uses a single levelset for each distinct grain or "material", including any substrate or any gas phase region above the grains. Using separate scalar fields for each distiguishable material does mean that the computational load scales with the number of distinct materials present in a given simulation. We use an MPI-based [31, 32] parallelization scheme allowing PLENTE to use up to N processor, where N is the number of materials in the simulation. We have run simulations for up to 128 material, on 64 processors. It should be noted that this does not limit the number of *grains* to N, rather only the number of distinct grain *orientations*. Grains with identical orientations do not form grain boundaries upon colliding.

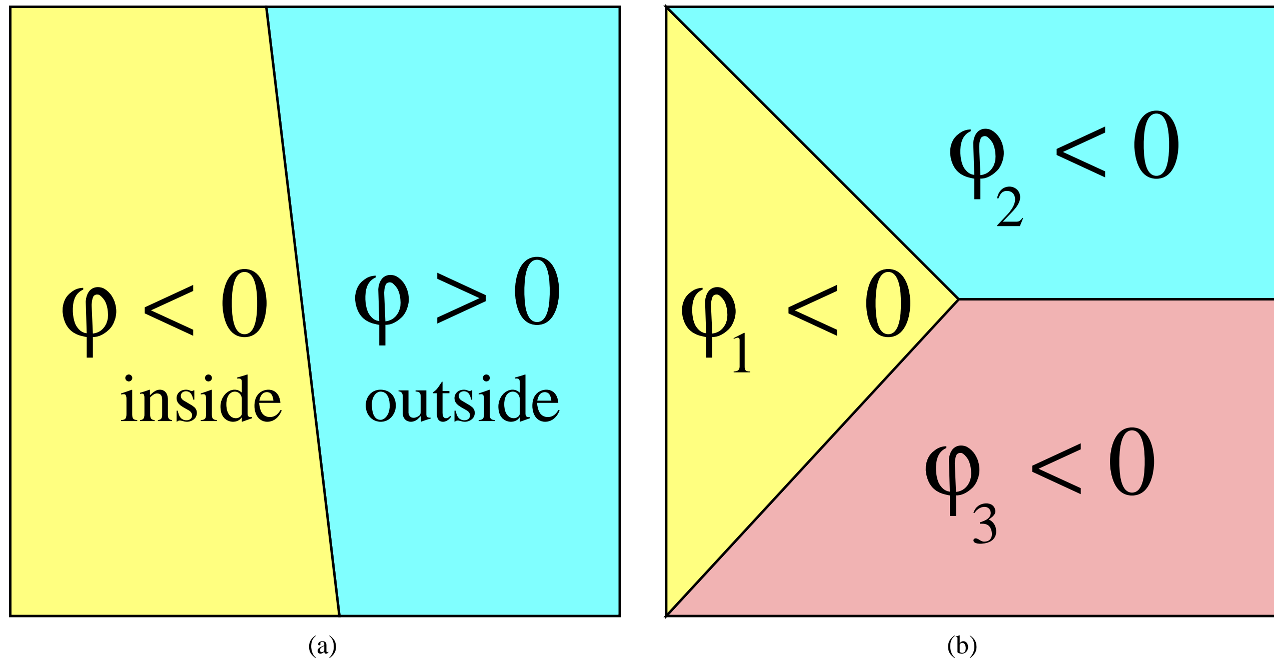

Figure 1. Sign convention for levelset scalar fields for (a) two-phase and (b) many-phase systems. Note that the number of phases is greater than the number of levelsets for two-phase systems and equal to the number of levelsets for many-phase systems.

2.2. Levelset Evolution

In implicit levelset representations, the evolution of the structure is reduced to the evolution of the field in which it is embedded, under the levelset equation [24, 25]:

$$\varphi_t + F\|\nabla\varphi\| = 0 \tag{1}$$

Equation (1) is of the Hamilton-Jacobi variety and can be solved by a variety of methods, including fast marching [25], finite difference approximations to the gradient with explicit time-stepping, and streamline upwinding Petrov Galerkin (SUPG) finite element methods [33]. `PLENTE` employs the SUPG method from Reference 33, adapted for unstructured tetrahedral meshes.

The quantity F from equation (1) is the "speed function" which represents a description of the speed at which the interface is moving in the direction normal to the surface. It is through this quantity that a process model or grain evolution model interfaces with `PLENTE`. `PLENTE` can provide a geometric structure to a process model, usually in the form of a surface mesh, along with geometric quantities associated with the elements of that mesh, such as curvature or grain boundary angle. From this information, the process model can calculate a velocity of this boundary which `PLENTE` can use to update the structure. For some levelset problems, most notably that of tracking interfaces between two fluids, F is defined away from the zero surface. In many cases such as deposition from a vapor phase, a process model in general only provides velocities on the surface, and they must be "extended" to the rest of the domain through one of a variety of methods [29, 34].

2.3. Reconciliation

As with any time stepping procedure, small errors occur due to the time discretization. However, with multiple levelset simulations, material-material interactions can occur in which the induced error is not physically realizeable [35]. This situation is analogous to physically unrealizeable structures that can result in explict front-tracking methods due to finite time step size. Figure 2 shows the development of a levelset "overlap". In this case it is necessary to reconcile the resulting levelsets. Reconcilation of the different levelsets is accomplished using the operator developed by Merriman, Bence, and

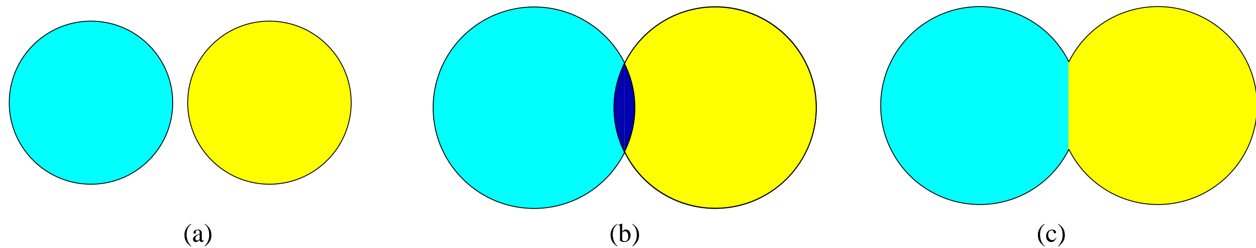

Figure 2. A schematic of how an overlap can develop and the resulting structure after reconciliation. (a) indicates an initial structure which due to a finite time step size, develops an "overlap" (the dark region in (b)) which is "inside" both materials. (c) After reconciliation, the overlap is no longer present and the system is physically realizable.

Osher in Ref. 35. This "MBO" operator is given by

$$\varphi_i^{\text{new}} = \varphi_i - \max_{j \neq i} \varphi_j \tag{2}$$

The form of the MBO reconcilation operator is semi-empirical and is motivated by the fact that it leaves equi-angular triple junctions evolving under mean curvature invariant, while being effective at removing overlaps and "void" regions during levelset interaction [35]. (Note: The term "void" as used here denotes a mathematical condition, and in the standard levelset interpretation, does not have a physical analogue. In particular, it does not denote a pocket of empty space, as might occur between grains.)

2.4. Re-initialization

Upon beginning a simulation and at certain times throughout, such as at the nucleation of a new phase, it is necessary to initialize a φ-field from scratch. The brute force method of finding and comparing distances from each entity making up an interface to each point on the mesh is prohibitive for complex surfaces or large meshes. Therefore we use the "closest point transform" (CPT) method reported by Mauch [36]. This method has the advantage of having optimal computational complexity, $O(m \cdot n)$, for a triangulated manifold surface of n faces and a mesh of m vertices. The CPT method involves selecting the small set of points in a tensor product grid to which an entity in the interface representation can possibly be closest. Figure 3 shows a how a two-dimensional domain can be divided into regions based on a piecewise segmented interface. The points on the regular grid that fall inside each region are easily identified and the distance to the interface calculated through explicit geometry.

After initializing points near the surfaces using the CPT method, we use standard fast marching techinques [25] to propagate signed distance and closest point information to the rest of the computational domain. We then interpolate that information onto our tetrahedral mesh. It is important to note that the CPT approach does not just provide distance information, but also provides the closest point on the surface to a given mesh node. We use this information when extending velocities off the interface. As shown in Richards *et al.* [29] for two dimensions, extending velocities using a closest point method can be made as accurate as more complicated approaches based on explicitly solving Riemann problems [28].

2.5. Encapsulation

Structural data from an atomistic simulation, such as that derived from a KLMC simulation, are often composed of positions of discrete particles. Each particle has a size associated with it, either explicitly or implicitly through its position on a lattice with a regular spacing. `PLENTE` finds an envelope (not necessarily convex) of the volume filled by these particle, or "encapsulates" them. In the case of data explicitly on lattices, the particle size is considered to be the size of the lattice cell, and no portion of the envelope is constructed between neighboring lattice sites occupied by the same particle type. Care is taken to preserve the partial volumes occupied by each phase, as well as the orientation of the underlying lattices. Figure 4a shows a data set taken from a two-lattice KLMC simulation of PVD of aluminum using `ADEPT` [10–12] in which the flat (100) phase competes with the pyrimidal (111) phase. Figure 4b shows the encapsulated version of these data (minus the underlying substrate).

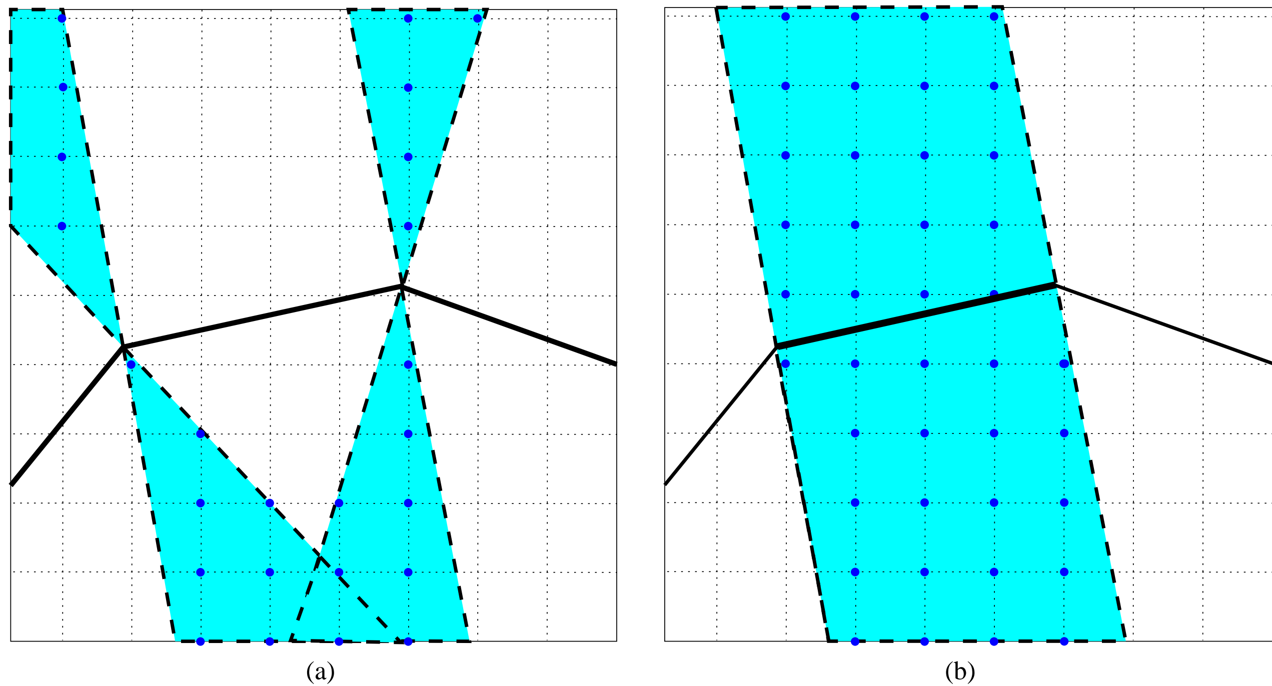

Figure 3. The division of a 2D domain into subdomains for the purposes of determining the points on an interface (dark solid line segments) closest to points on a regular grid. In (a), the set of points that could possibly have their closest point on the interface be the two vertices of the interface is shaded. In (b), the set of points with closest points on the central segment is shaded. In both cases, the points on the underlying regular grid inside these subdomains are highlighted.

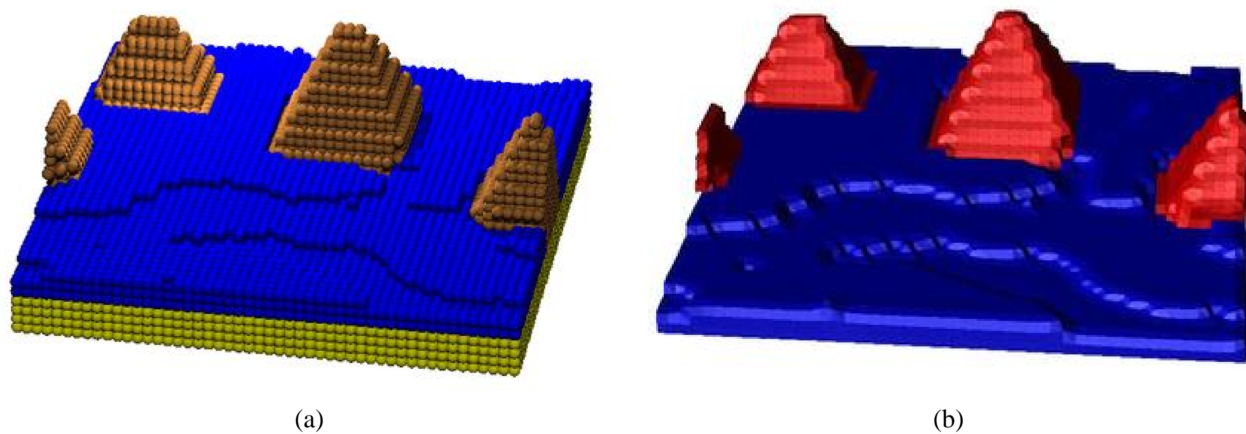

Figure 4. (a) Results of a kinetic lattice Monte Carlo simulation of physical vapor deposition of aluminum using `ADEPT` [10–12] with two lattices. The flat (100) phase competes with the pyrimidal (111) phase. (b) The encapsulated version of the data shown in (a) (minus the underlying substrate).

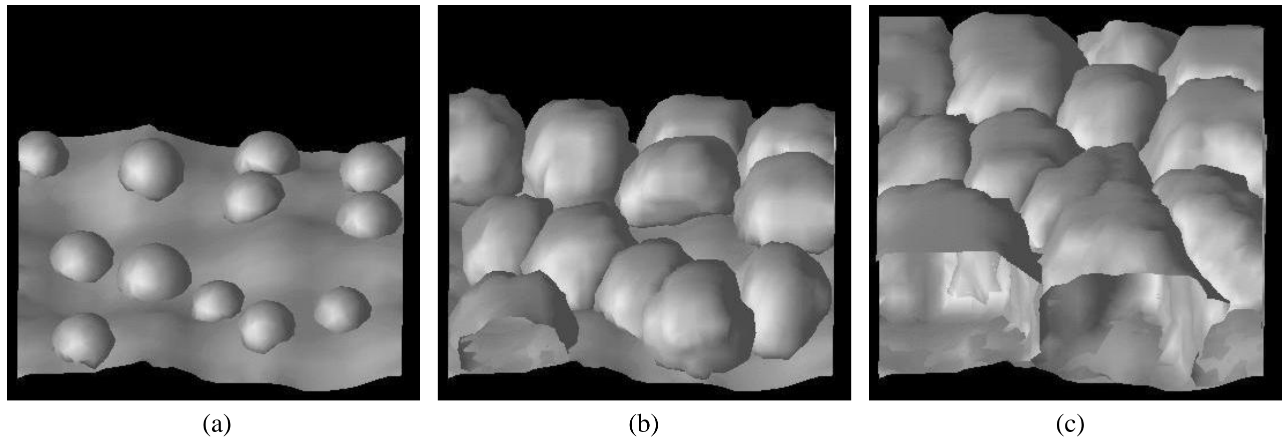

Figure 5. An evolving set of islands growing and coalescing into a blanket film under kinetically limited electroless deposition with a 10% noise term as noted in the text.

Atomic positions combined with an assumed particle size can give rise to non-physical situation, in which one particle penetrates another. Although encapsulation is best reserved for systems of a scale at which addition or deletion of a single particle is negligible, a resolution of the non-physical situation is necessary. In this case, `PLENTE` simply allows the interpenetration to exist in an initial levelset representation, and then reconciles all the levelsets to eliminate such overlaps.

3. RESULTS

`PLENTE` is designed to be a very general geometry tracker, enabling it to be used with a wide variety of process models. As discussed in section 2.2, all that is required is an ability to calculate an interface velocity as a function of geometry. We have used this software environment to track structure for a variety of process models. Here, we review some of the results of the selected process models.

3.1. Electroless Deposition

One simple, physically realistic model available is electroless deposition (ELD) of metal in a kinetically limited regime. By choosing a kinetically limited process we eliminate questions of transport from the calculation and highlight the three dimensional shape evolution and material interaction. This model yields bimodal velocities for each material: the average deposition rate for the free surface, and zero for subsurface material boundaries, such as where a grain meets a substrate, or a grain boundary has formed.

Tseng *et al.* [37, 38] reported data on a HNO_3–$CuCl_2$ bath for copper deposition which includes several SEM micrographs of copper islands before coalescence into a blanket film. Visual inspection indicates that islands are all approximately within a factor of two in radius, indicating an initial period of nucleation followed by nucleation free growth. We have modeled this, assuming an initial set of hemispherical nuclei, approximately normally distributed around a central size, and placed on the substrate randomly, such that no two islands impinge on each other in the initial condition. The kinetics at the free surface are the same on each island, giving isotropic evolution of the free surfaces. The micrographs from Reference 37 show that many of the resulting grains are close to spherical, and thus we feel that this essentially isotropic model is a reasonable starting point.

We placed our simulated islands on a slightly rough (5 nm rms roughness) substrate as shown in Figure 5a. We have specified natural boundary conditions at the domain sidewalls. Figures 5b and c show the evolution of our set of islands, using the ELD process model. A small (10%) noise term has been introduced to the surface velocity to mimic local fluctuations in deposition rate. As the islands grow, they begin to impinge on one another and form grain boundaries, until a fully coalesced, blanket film exists, as shown in Figure 5c. At this point, the resulting grain structure may be the subject of further processing, or used as input to a continuum-based property calculation model.

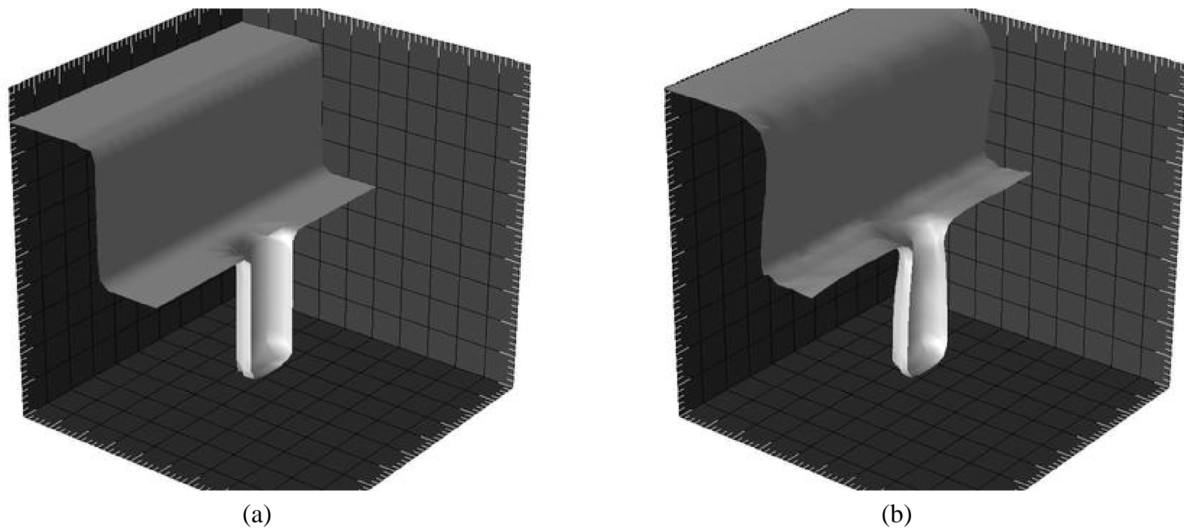

(a) (b)

Figure 6. (a) Cross sectioned view of starting substrate for the first physical vapor deposition simulation described in the text. This dual damascene structure consists of a 2.0 aspect ratio via at the bottom of a 1.15 aspect rato rectangular trench of the same depth as the via. (b) Film surface after physical vapor deposition of 140 nm barrier layer. The film thickness drops to under 10 nm at the edge of the via bottom.

3.2. Physical Vapor Deposition

We have also simulated physical vapor deposition (PVD), which in contrast to the ELD model discussed above, is modelled as being transport limited, having a sticking factor of unity. For deposition systems with high Knudsen numbers, *i.e.*, for structures with length scales of interest that are significantly smaller than the mean free path, transport is by line-of-sight and is dominated by particle-structure collisions (as opposed to particle-particle collisions) [39, 40]. Thus, flux to the surface can be calculated using a flux distribution from the source volume above the substrate and a set of "view factors" calculated solely from the geometry of the structure.

We use a view factor code that employs a Monte Carlo method to sample the differential transmission probability distributions between the triangles which define a surface mesh describing the geometry of the system and a source plane placed above the surface. Using this code with `PLENTE` and applying a Maxwellian flux distribution at the source plane, we simulate deposition of a 140 nm thick barrier film into a representative "dual damascene" structure shown in Figure 6a). Periodic boundary conditions are applied in directions transverse to the plane of the substrate. Figure 6b shows the resulting film, which exhibits significant bottlenecking at the top of the via structure, limiting the thickness to under 10 nm at the bottom corner of the via. This simulation highlights the usefulness of the ability to represent structures and simulate transport in three dimensions. It should be noted that although such three dimensional simulations are informative and provide information not provided by two dimensional simulations, comparison with experimental data can be limited.

Although it may be interesting to simulate deposition of continuous films, PVD can give rise to film rich in microstructure, as shown by the SEMs of the tantalum oxide film imaged in Figure 7. To investigate such microstructure, we used a KLMC code, described in Reference 41, to develop an initial set of nucleated islands (shown in Figure 8a. We then used `PLENTE`'s encapsulation routines and evolved the structure (see Figures 8b, c, and d), using a Maxwellian distribution of flux from the source and a unity sticking factor. The structure shown in Figure 8d represents 500 steps, recalculating view factors every 10 steps and took 3 hours on 18 processors of a Beowulf cluster. After an initial period of non-interacting growth, grains begin to significantly shadow their neighbors, resulting in very vertical growth that gives rise to the columnated structure seen in Figure 8d. The columnar structure that results exhibits quite stable void spaces near the substrate and near vertical triple lines due to shadowing in these regions. For some deposition processes, it might be necessary to augment the line-of-sight model with surface diffusion and/or grain boundary migration terms. Although the simulation results shown in Figure 8 do not agree in detail with the SEMs in Figure 7, it seems clear that such SEMs and cross sectional SEMs can be used to test transport and reaction models as is routinely done with topography simulation [42,43].

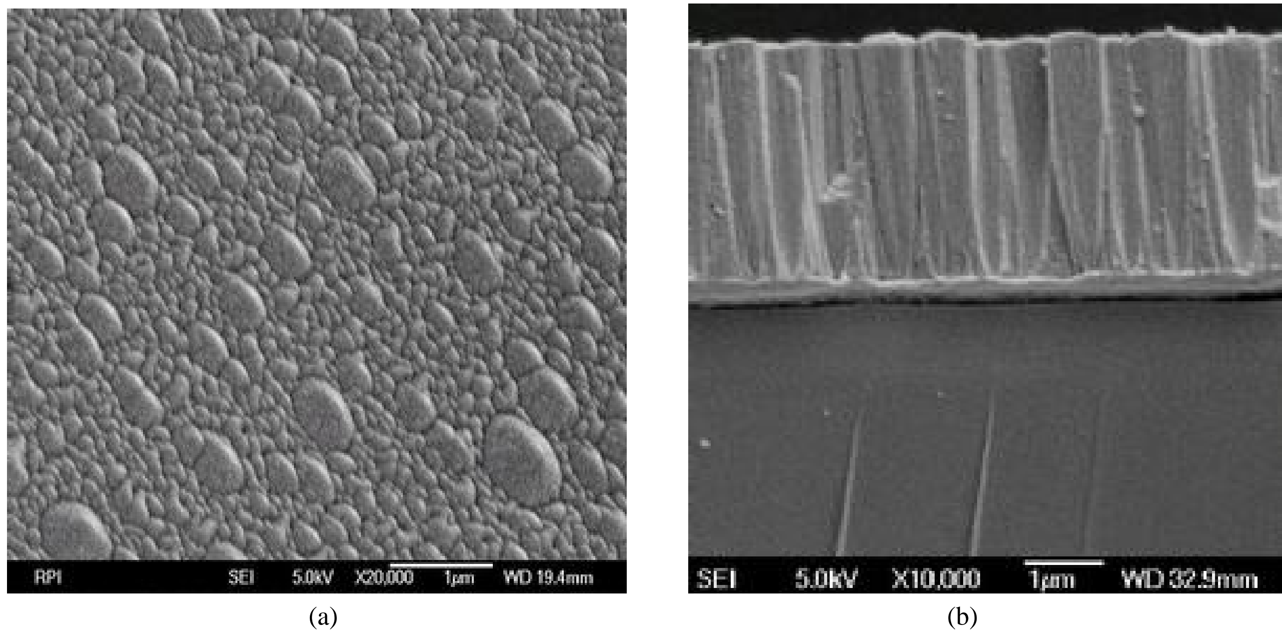

(a) (b)

Figure 7. SEM image of a TaO_x film deposited via reactive sputtering, (a) imaged at a 10° angle from plan view, and (b) in cross section.

As a final example, and one that is neither kinetically nor transport limited, we demonstrate the use of PVD exhibiting anisotropic growth kinetics. We begin with the same starting structure as shown in Figures 8a and b for simple PVD, orienting each island randomly, but with a <111> texture. Fluxes are calculated to the surface as above, but the unity sticking factor on each face is multiplied by projecting a unit normal along the [111] vectors relative to the assigned grain orientation. This give a unity sticking factor on {111} sections of the surface, but a sticking factor of only 0.58 on the {100} surfaces. Figure 9 shows the resulting structure, which differs significantly from the unity sticking factor result, displaying distinctly pyrimidal shapes at the top of square columns. The faces of these pyramids correspond to {100} planes.

4. CONCLUSIONS

Grain-continuum representation and tracking of microstructural systems can be a powerful method for simulating the development and evolution of grain structures. We believe grain-continuum codes such as `PLENTE` can complement discrete representation methods such as kinetic lattice Monte Carlo techniques by extending the length scales accessible to computation. Techniques exist and continue to be developed to move efficiently from discrete to continuum and vice versa, in order to automate using discrete inputs to codes such as `PLENTE`. For systems in which models of nucleation or island formation already exist for pre-coalescence, `PLENTE` can be used to follow the system through coalescence to the blanket film stage. Though we have not discussed the need to go from continuum to discrete models, we anticipate the need to regenerate atomistic representations of parts of grain-continuum representations, in order to develop more appropriate transport models for grain boundaries and surfaces.

We have presented selected process models that have been used with our grain-continuum code, including a simple kinetically limited electroless deposition as well as a physical vapor deposition starting from a structure encapsulated from a KLMC simulation, and an aniostropic growth model. Very different process models were chosen to demonstrate the wide applicability of the presented technique, and application to other process models is underway.

5. ACKNOWLEDGMENTS

The authors thank Leonard J. Borucki, Dibyendu Datta, Andrew Kuprat, Kenneth E. Jansen, Ottmar Klaas, and Mark S. Shephard for useful discussions and Pushkar Jain for the use of his TaO_x SEM. We acknowledge MARCO, DARPA, and

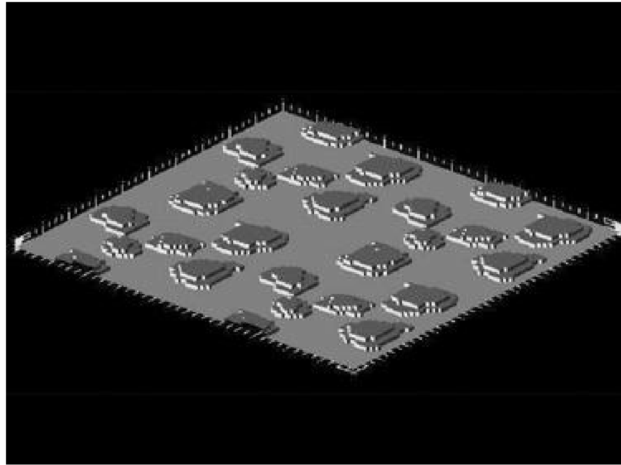

(a)

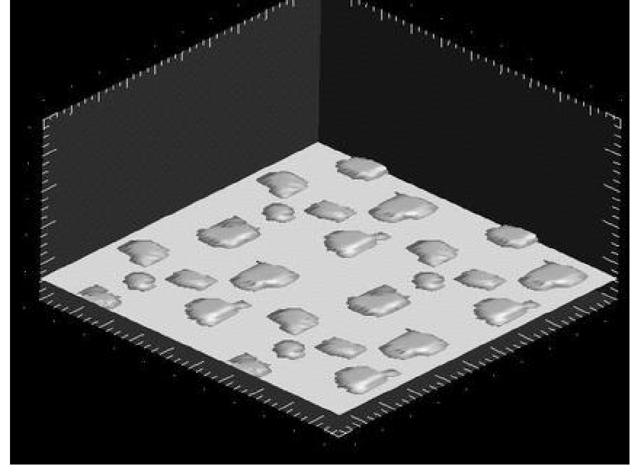

(b)

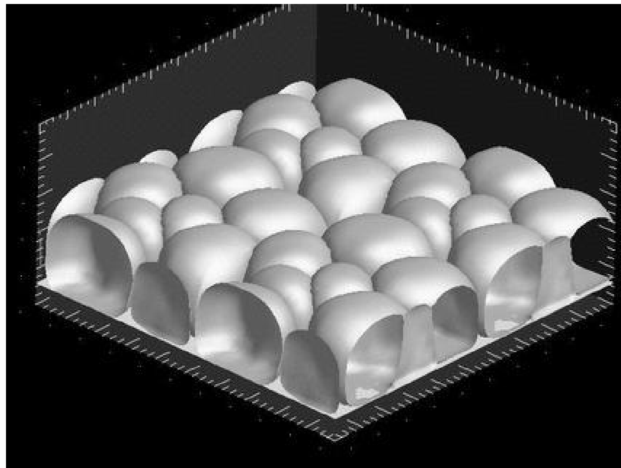

(c)

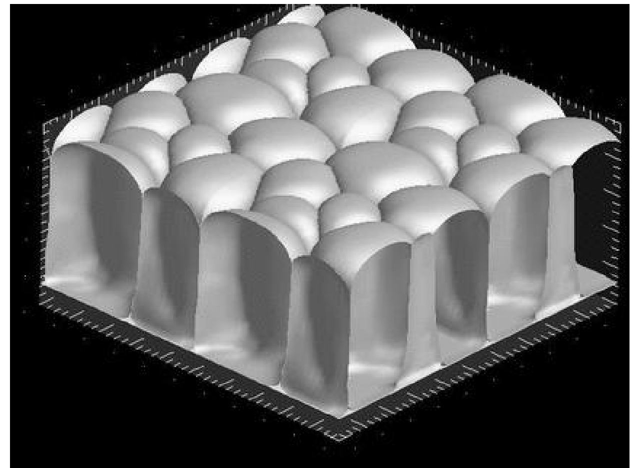

(d)

Figure 8. (a) The discrete data taken from a kinetic lattice Monte Carlo simulation of physical vapor deposition, in the initial islanding stage. (b) Encapsulation of (a), used as the starting structure for a grain continuum based PVD simulation. (c) and (d) later stages in the grain continuum based simulation, after coalescence of islands.

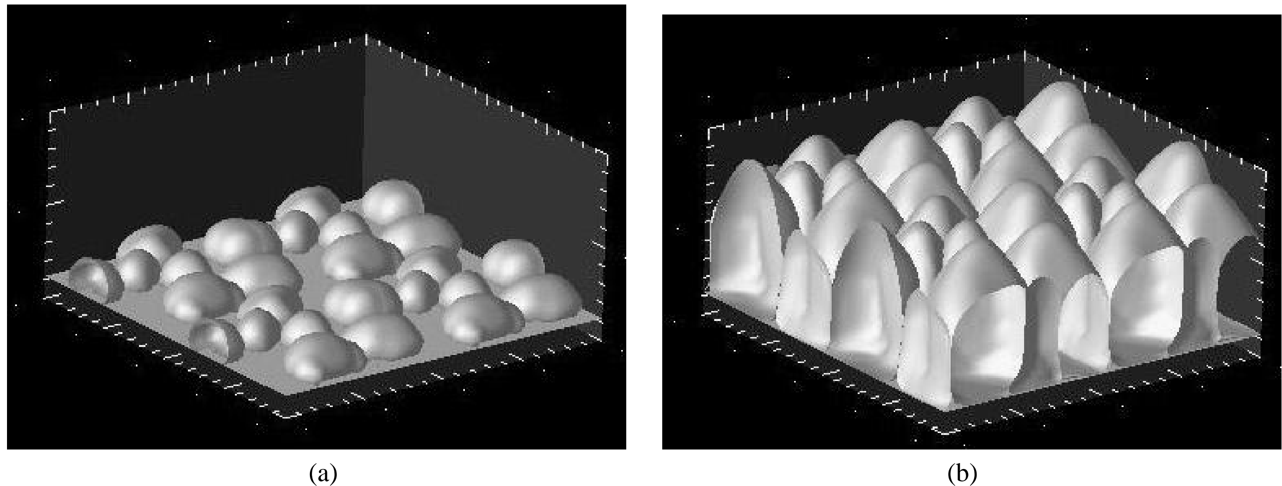

(a) (b)

Figure 9. The later stages of a PVD simulation with anisotropic kinetics, yielding preferential growth directions. Grains have <111> texture and higher sticking factors in [111] directions, as discussed in the text. (a) Developing structure, before coalescence into blanket film. (b) Structure after coalescense exhibiting distinct {100} surfaces. Initial structure is as in Figure 8.

NYSTAR for their support of this work through the Focus Center—New York, Rensselaer: Interconnections for Gigascale Integration.

REFERENCES

1. C. Seah, S. Mridha, and L. Chan, "Quality of electroplated copper films produced using different acid electrolytes," *J. Vac. Sci. Technol. B* **17**, pp. 2362–2356, Sept. 1999.
2. P. Besser, E. Zschech, W. Blum, D. Winter, R. Ortega, S. Rose, M. Herrick, M. Gall, S. Thrasher, M. Tiner, B. Baker, G. Braeckelmann, L. Zhao, C. Simpson, C. Capasso, H. Kawasaki, and E. Weitzman, "Microstructural characterization of inlaid copper interconnect lines," *J. of Electron. Mat.* **30**, pp. 320–330, Apr. 2001.
3. A. Fischer, A. von Glashow, A. Huot, and R. Schwarzer, "Crystal texture of electroplated damascene Cu interconnects," in *Advanced Metallization Conference 1999 (AMC 1999)*, M. Gross, T. Gessner, N. Kobayashi, and Y. Yasuda, eds., pp. 137–141, Mater. Res. Soc., (Warrendale, PA, USA), 1999.
4. V. Dubin, C. Thomas, N. Baxter, C. Block, V. Chikarmane, P. McGregor, D. Jentz, K. Hong, S. Hearne, C. Zhi, D. Zierath, B. Miner, M. Kuhn, A. Budrevich, H. Simka, and S. Shankar, "Engineering gap fill, microstructure and film composition fof electroplated copper for on-chip metallization," in *Proc. IEEE 2001 Intl. Interconnect Tech. Conf.*, pp. 271–273, IEEE, (Piscataway. NJ), 2001.
5. Y. Morand, "Copper metallization for advanced IC: requirements and technological solutions," *Microelectron. Eng.* **50**, pp. 391–401, Jan. 2000.
6. P. S. Sahni, D. J. Srolovitz, G. S. Grest, M. P. Anderson, and S. Safran, "Kinetics of ordering in two dimensions. II. quenched systems," *Phys. Rev. B* **28**, pp. 2705–2716, Sep. 1983.
7. G. S. Grest, M. P. Anderson, and D. J. Srolovitz, "Comparison of domain growth kinetis in two and three dimensions," in *Time-Dependent Effects in Disordered Materials*, R. Pynn and T. Riste, eds., *NATO ASI Series B: Physics*, Plenum Press, 1987.
8. M. T. Lusk, "A phase-field paradigm for grain growth and recrystallization," *R. Soc. London A* **455**, pp. 677–700, Feb 1999.
9. B. Schonfelder, D. Wolf, S. Philpot, and M. Furtkamp, "Molecular-dynamics for the simulation of grain-boundary migration," *Interface Sci.* **5**, pp. 245–262, Nov 1997.
10. H. Huang, G. Gilmer, and T. D. de la Rubia, "An atomic simulator for thin film deposition in three dimensions," *J. Appl. Phys* **84**, pp. 3636–3649, Oct. 1998.
11. H. Huang and G. Gilmer, "Atomistic simulation of texture competition during thin film deposition," *J. of Computer-Aided Mat. Des.* **7**(3), pp. 203–216, 2000.

12. H. Huang and G. Gilmer, "Texture competition during thin film deposition — effects of grain boundary migration," *Comp. Mat. Sci.* **23**, pp. 190–196, 2002.
13. H. Frost and C. Thompson, "Computer simulation of microstructural evolution in thin films," *J. of Electron. Mat.* **17**, pp. 447–458, Sept. 1988.
14. H. Frost, C. Thompson, and D. Walton, "Simulation of thin film grain structures. I. grain growth stagnation," *Acta Metall. Mater* **38**(8), pp. 1455–1462, 1990.
15. J. Zhang and J. Adams, "FACET: a two dimensional simulator of polycrystalline thin film growth," in *Multiscale Modeling of Materials*, L. Kubin, R. Selinger, J. Bassani, and K. Cho, eds., *Mater. Res. Soc. Symposium Proceedings* **653**, pp. Z10.1.1–6, Mater. Res. Soc., 2000.
16. A. Roosen and W. Carter, "Simulations of microstructural evolution: anisotropic growth and coarsening," *Physica A* **261**(1–2), pp. 232–247, 1998.
17. A. Kuprat, "Modeling microstructure evolution using gradient-weighted moving finite elements," *SIAM Journal on Scientific Computing* **22**, pp. 535–560, July 2000.
18. "LaGriT: The Los Alamos grid toolbox." http://www.t12.lanl.gov/ lagrit/.
19. A. Kuprat, "Adaptive smoothing techniques for 3-d unstructured meshes," 1996. LA-UR-96-1116, Los Alamos National Laboratory.
20. A. Kuprat and D. George, "Maintaining tetrahedral mesh quality in response to time-dependent topological and geometrical deformation," in *Proc. of 6th Int. Conf. on Num. Grid Generation in Comp. Field Simulations*, M. Cross, ed., pp. 589–598, Intl. Soc. of Grid Generation, 1998.
21. A. Kuprat, D. George, E. Linnebur, H. Trease, and R. K. Smith, "Moving adaptive unstructured 3-D meshes in semiconductor process modelling applications," *VLSI Design* **6**(1-4), pp. 373–378, 1998. LA-UR-95-4128.
22. D. George, N. Carlson, J. T. Gammel, and A. Kuprat, "3D modeling of metallic grain growth," in *Proceedings of Modeling and Simulation of Microsystem*, M. Laudon, ed., pp. 463–466, 1999. LA-UR-99-986, Los Alamos National Laboratory.
23. A. Kuprat, "Inspecting and repairing physical topology in a moving grid grain growth simulation," July 2000. LA-UR-00-3475, Los Alamos National Laboratory.
24. S. Osher and J. Sethian, "Fronts propogating with curvature dependent speed: Algorithms based on Hamilton-Jacobi formulations," *J. Comp. Phys* **79**, pp. 12–49, 1988.
25. J. A. Sethian, *Level Set Methods and Fast Marching Methods*, no. 3 in Cambridge Monographs on Applied and Computational Mathematics, Cambridge University Press, Cambridge, UK, 2nd ed., 1999.
26. M. O. Bloomfield, D. F. Richards, and T. S. Cale, "A computational framework for modeling grain structure evolution in three dimensions," *Phil. Mag. A* , 2003. revised.
27. G. Russo and P. Smereka, "A level-set method for the evolution of faceted crystals," *SIAM J. Sci. Comput.* **21**(6), pp. 2073–2095, 2000.
28. D. S. Ross, "Evolution of material boundaries under ion bombardment," *J. Electrochem. Soc.* **135**, pp. 1260–1265, May 1988.
29. D. F. Richards, M. O. Bloomfield, S. Sen, and T. S. Cale, "Extension velocities for level set based surface profile evolution," *J. Vac. Sci. Technol. A* **19**, pp. 1630–1635, Jul/Aug 2001.
30. D. Enright, R. Fedkiw, J. Ferziger, and I. Mitchell, "A hybrid particle level set method for improved interface capturing," *J. Comp. Phys.* **183**, pp. 83–116, Nov 2002.
31. "The message passing interface (MPI) standard." http://www-unix.mcs.anl.gov/mpi/.
32. P. S. Pacheco, *Parallel Programming with MPI*, Morgan Kaufmann Publishers, Inc., San Fransisco, 1997.
33. T. J. Barth and J. A. Sethian, "Numerical schemes for the Hamilton-Jacobi and level set equations on triangulated domains," *J. Comp. Phys* **145**, pp. 1–40, Jan. 1998.
34. D. Adalesteinsson and J. A. Sethian, "The fast construction of extension velocities in level set methods," *J. Comp. Phys* **148**, pp. 2–22, 1999.
35. B. Merriman, J. K. Bence, and S. J. Osher, "Motion of multiple junctions: A level set approach," *J. Comp. Phys* **112**, pp. 334–363, 1994.
36. S. Mauch, "A fast algorithm for computing the closest point and distance transform." http://http://www.acm.caltech.edu/ seanm/software/cpt/cpt.pdf, April 2000.

37. W.-T. Tseng, C.-H. Lo, and S.-C. Lee, "Electroless deposition of cu thin films with $CuCl_2$-HNO_3 based chemistry: I. chemical formulation and reaction mechanisms," *J. Electrochem. Soc.* **148**, pp. C327–C332, May 2001.
38. W.-T. Tseng, C.-H. Lo, and S.-C. Lee, "Electroless deposition of cu thin films with $CuCl_2$-HNO_3 based chemistry: II.kinetics and microstructure," *J. Electrochem. Soc.* **148**, pp. C333–C338, May 2001.
39. T. S. Cale and G. B. Raupp, "Free molecular transport and deposition in cylindrical features," *J. Vac. Sci. Technol. B* **8**, pp. 649–655, Jul/Aug 1990.
40. T. S. Cale and G. B. Raupp, "A unified line-of-sight model of deposition in rectangular trenches," *J. Vac. Sci. Technol. B* **8**, pp. 1242–1248, Nov/Dec 1990.
41. A. Challa, J. Drucker, and T. Cale, "Morphology of Ag islands grown on GaAs(110) at low coverage: Monte Carlo simulations," in *Evolution of Epitaxial Structure and Morphology*, A. Zangwill, D. Jesson, D. Chambliss, and R. Clarke, eds., *MRS Proceedings* **399**, pp. 103–108, Mat. Res. Soc., 1996.
42. T. S. Cale and V. Mahadev, *Modeling of Film Deposition for Microelectronic Applications*, vol. 22 of *Thin Films*, ch. 4, pp. 175–276. Academic Press, San Diego, CA, 1996.
43. T. P. Merchant, M. K. Gobbert, T. S. Cale, and L. J. Borucki, "Topography simulation for the virtual wafer fab," *Thin Solid Films* **365**(2), pp. 368–375, 2000.